Check for updates

Research Article

Multi-Well Array Culture of Primary Human Hepatocyte Spheroids for Clearance Extrapolation of Slowly Metabolized Compounds

Lena C. Preiss,[1,2] **Volker M. Lauschke,**[2,3,4] **Katrin Georgi,**[1] **and Carl Petersson**[1,5]

Abstract. Accurate prediction of human pharmacokinetics using *in vitro* tools is an important task during drug development. Albeit, currently used *in vitro* systems for clearance extrapolation such as microsomes and primary human hepatocytes in suspension culture show reproducible turnover, the utility of these systems is limited by a rapid decline of activity of drug metabolizing enzymes. In this study, a multi-well array culture of primary human hepatocyte spheroids was compared to suspension and single spheroid cultures from the same donor. Multi-well spheroids remained viable and functional over the incubation time of 3 days, showing physiological excretion of albumin and α-AGP. Their metabolic activity was similar compared to suspension and single spheroid cultures. This physiological activity, the high cell concentration, and the prolonged incubation time resulted in significant turnover of all tested low clearance compounds ($n = 8$). In stark contrast, only one or none of the compounds showed significant turnover when single spheroid or suspension cultures were used. Using multi-well spheroids and a regression offset approach ($\log(CL_{int}) = 1.1 \times + 0.85$), clearance was predicted within 3-fold for 93% (13/14) of the tested compounds. Thus, multi-well spheroids represent a novel and valuable addition to the ADME *in vitro* tool kit for the determination of low clearance and overall clearance prediction.

[1] Department of Drug Metabolism and Pharmacokinetics (DMPK), The Healthcare Business of Merck KGaA, Frankfurter Str. 250, 64293, Darmstadt, Germany.

[2] Department of Physiology and Pharmacology, Karolinska Institutet, Stockholm, Sweden.

[3] Dr Margarete Fischer-Bosch Institute of Clinical Pharmacology, Stuttgart, Germany.

[4] University of Tuebingen, Tuebingen, Germany.

[5] To whom correspondence should be addressed. (e–mail: carl.petersson@emdserono.com)

Abbreviations: *α-AGP*, α1-acid glycoprotein; *AAFE*, Absolute average fold error; *ADME*, Absorption, distribution, metabolism, excretion; *CL_int*, Intrinsic clearance; *CL_int,obs*, Observed intrinsic clearance; *CL_int,pred*, Predicted intrinsic clearance; *CL_b*, *In vivo* clearance; *CL_b,obs*, Observed *in vivo* clearance; *CL_b,pred*, Predicted *in vivo* clearance; *CYP*, Cytochrome P450; *FBS*, Fetal bovine serum; *fu_b*, Fraction unbound in blood; *fu_inc*, Fraction unbound in the incubation; *fu_p*, Fraction unbound in plasma; *IVIVE*, *In vitro-in vivo* extrapolation; *LOOCV*, Leave one out cross-validation; *MPCCs*, Micropattern co-cultures; *PHH*, Primary human hepatocytes; *pl*, Plasma; *Q_h*, Liver blood flow; *R_b*, Blood-to-plasma ration; *UGT*, Uridine 5'-diphosphoglucuronosyltransferase; *ULA*, Ultra-low attachment; *WSM*, Well-stirred model.

INTRODUCTION

High-throughput ADME screening and improved *in silico* tools have facilitated the identification of an increasing number of compounds with low intrinsic clearance (CL_{int}) in drug discovery (1). However, predicting the clearance of slowly metabolized compounds is frequently challenging as microsomes show rapidly declining activity limiting incubation times to less than 1 h. Functionality of primary human hepatocytes (PHH) in suspension culture is slightly more stable and activity of drug metabolizing enzymes declines within few hours (2–4). Cell lines like HepG2 and HepaRG cells and induced pluripotent stem cell (iPSC)-derived hepatocyte-like are viable for extended periods and have therefore been tested as an alternative for CL_{int} determinations. Drug metabolizing enzymes in HepG2 and iPSC-derived hepatocyte-like cells have been shown to be less active compared to suspension cultures and are therefore not suitable for low clearance determinations (5). Although HepaRG cells have been shown to be similarly active as suspension cultured PHH, measured CL_{int} values were lower (5, 6). Therefore, alternative culture methods like repeated suspension cultures (relay method) and more advanced cell culture models using PHH have been suggested to determine

low CL_{int} compounds (7–10). For the relay method, whole supernatant from suspension cultures is collected and re-incubated with fresh suspension cultures thereby extending the total incubation time. This method is however relatively laborious and technically challenging. Advanced cell culture models, such as micropatterned co-cultures (MPCC) and liver spheroids, provide alternate means to extend the incubation time as hepatocytes viability and function is preserved. These methods are less laborious and easier to perform compared to the relay method and are therefore more widely used. Kratochwil *et al.* reported predicted clearance within 2-fold of *in vivo* clearance for the majority of nine low clearance compounds when using MPCCs (5). In contrast, CL_{int} for only 2 out of 5 low clearance compounds were predicted within 3-fold using static 2D co-cultures of PHH and stromal cells (6). In another study by Hultman *et al.*, 50% (7/14) of the low clearance compounds were predicted within 2-fold when 2D co-cultures were used (11).

Liver spheroid cultures retain their physiological transcriptomic, proteomic, and metabolomic signatures and remain metabolic active for multiple weeks (12, 13). These cultures have been successfully used for toxicology studies and modeling of human liver diseases (14). Furthermore, their physiologically relevant phenotype has rendered interest for their use in drug metabolism and pharmacokinetic studies (15). Due to their functional stability, human liver spheroids allow for long incubation times. Their use for low clearance compounds has however been limited by low cell concentrations required in these cultures (16, 17).

Here, we present PHH spheroids in multi-well arrays in which up to 80 spheroids can be cultured per well as spatially separated, fully functional units, thus achieving high cell concentrations while maintaining activity of drug metabolizing enzymes for extended periods of time. We compared critical endpoints such as detection limit and extrapolation to *in vivo* clearance of PHH spheroid cultures in multi-well arrays to isogenic single spheroid and suspension cultures from the same donor, using eight low clearance and six intermediate to high clearance compounds with different metabolic routes.

MATERIALS AND METHODS

Materials

William's E medium, L-glutamine-penicillin-streptomycin solution, midazolam, 1'OH-midazolam, 4'OH-diclofenac, dextrorphan, dextromethorphan, amodiaquine, *N*-desethyl-amodiaquine, dexamethasone, 7'OH-coumarin, 7'OH-coumarin glucuronide, Trypan blue, and acetonitrile were purchased from Sigma-Aldrich (St. Louis, MO, USA). Elplasia 96-well round bottom ultra-low attachment (ULA) plates, 96-well clear round bottom ULA plates, and 96-well white round bottom polystyrene microplates were purchased from Corning (Glendale, AZ, USA). Fetal bovine serum was obtained from Cytiva (Marlborough, MA, USA). The CellTiter-Glo Luminescent Cell Viability kit was purchased from Promega (Madison, WI, USA). Insulin-transferrin-selenium solution and rapid equilibrium dialysis plates were obtained from Thermo Fisher Scientific (Waltham, MA, USA). Cryopreserved primary human hepatocytes (Lot

HJK), INVITROGRO Krebs-Henseleit Buffer, INVITROGRO HT medium, INVITROGRO CP medium, and TORPEDO antibiotic mix were purchased from BioreclamationIVT (NY, USA). Acetaminophen, phenacetin, diclofenac, theophylline, metoprolol, etodolac, ondansetron, ketoprofen, tolbutamide, warfarin, lorazepam, chlorpromazine, propranolol, nifedipine, verapamil, metoprolol, naloxone, and glipizide were provided by the compound management department of Merck KGaA (Darmstadt, Germany).

Cell Culture

All experiments were performed using cryopreserved PHH from a single donor (lot HJK; BioreclamationIVT). Specific donor information can be found in Supplemental Table 1. For suspension culture, PHH were thawed, and incubations were performed with a total number of 0.5 million cells in 100 µL of Krebs-Henseleit buffer (pH 7.4) as previously reported (18). Compound concentration of 1 µM was used and plates were gently agitated during the incubation.

Single spheroid cultures were formed as previously described (12). In short, PHH were thawed and seeded in 96-well ULA plates at densities of 1500 cells/well. Subsequently, spheroids were cultured in PHH medium (William's E medium supplemented with 2 mM L-glutamine, 100 units/mL penicillin, 100 µg/mL streptomycin, 10 µg/mL insulin, 5.5 µg/mL transferrin, 6.7 ng/mL sodium selenite, and 100 nM dexamethasone) supplemented with 10% fetal bovine serum (FBS). After 5 days, the formed spheroids were shifted to serum-free PHH medium. On day 7, incubation with test compounds at a concentration of 1 µM was started in 100 µL of serum-free PHH medium.

For multi-well spheroid cultures, plates with ~ 80 microwells per macrowell were prewetted with 50 µL PHH medium supplemented with 10% FBS. Subsequently, PHH were seeded in 100 µL medium at a density of 40,000 cells per macrowell, resulting in an average cell number of 500 cells per spheroid. As with single spheroids cultures, formed spheroids were shifted to serum-free PHH medium after 5 days and incubation with 1 µM of test compound was initiated on day 7 in 150 µL of serum-free PHH medium.

Probe substrates for metabolic activity measurements were incubated in a cocktail (Table I). UGT activity was measured by incubation 100µM of substrate 7'OH-coumarin. All incubations were carried out in duplicate at 37°C, 5% CO_2 and 100% humidity.

Viability, Albumin, and α-AGP Measurements

Cell viability was assessed by quantification of intracellular ATP levels using the CellTiter-Glo Luminescent Cell Viability Assay (Promega) at different timepoints as indicated. Spheroids from one macrowell were transferred in 50 µL medium to the measurement plate, mixed 1:1 with ATP reagent and the solution was agitated at 450 rpm for 30 min at room temperature before luminescence was measured. Human albumin and α_1-acid glycoprotein (α-AGP) ELISA kits were purchased from Abcam (Cambridge, UK) and

Table I. Probe Substrate Cocktail for CYP Activity Measurements

CYP	Probe substrate	Concentration in incubation [μM]	Metabolite
CYP3A4	Midazolam	10	1-Hydroxy Midazolam
CYP2C8	Amodiaquine	10	N-Desethyl Amodiaquine
CYP1A2	Phenacetin	50	Acetaminophen
CYP2C9	Diclofenac	10	4-Hydroxy Diclofenac
CYP2D6	Dextromethorphan	5	Dextrorphan

measurements were conducted according to the manufacturer's instructions.

LC-MS/MS Analysis

Samples were taken at different time points and stopped with double the volume of ice-cold acetonitrile containing 3 μM of the internal standard pruvanserin. Samples were kept at – 80 °C until further use. The plates were centrifuged for 30 min at 3500 g at 4 °C and samples were diluted 1:10 with 66% acetonitrile before LC-MS/MS analysis.

LC-MS/MS analysis was performed with an AB Sciex API 6500+ triple quadrupole (AB Sciex LLC, MA, USA) coupled with a Waters Acquity I-Class UPLC (Waters Corporation, MA, USA). The software Analyst v1.7 (AB Sciex LLC) was used for control. An Acquity UPLC BEH C18 1.7 μm, 2.1 mm × 50 mm column (AB Sciex LLC) was used. Mobile phase A was 70 mM ammonium formate buffer containing 0.1% (v/v) formic acid and B was acetonitrile.

Aliquots (4 μL) of the centrifuged samples were injected. The gradient conditions were the following: 0–0.1 min 0% B, 0.1–0.8 min 0–100% B, 0.8–1.0 min 100% B, 1.0–1.4 min 0% B. The flow rate was 0.8 mL/min and data collection occurred between 0.3 and 1.4 min. Electrospray ionization in positive or negative mode with multiple reaction monitoring was used. The parameter settings are summarized in Supplemental Table 2. The formation rate of the respective metabolites was calculated and corrected for cell concentration. To compare cytochrome P450 (CYP) activity measurements, a one-way ANOVA followed by a Tukey-Kramer test was performed.

Determination of Fraction Unbound in Plasma

The unbound fraction in plasma (fu_p) was determined by equilibrium dialysis in the RED device (Thermo Fisher Scientific) using concentrations of 1 μM. Human plasma was dialyzed against phosphate buffer at pH 7.4 for 4 h. After

Table II. Compound Properties Including Ion Class, R_b, Fraction Unbound in Plasma (fu_p) and Fraction Unbound in the Incubation (fu_{inc})

Compound	Ion Class	Main metabolizing enzymes	R_b	fu_p	fu_{inc}			
					Measured fu_{inc}*	Suspension	Single spheroids	Multi-well
low CL$_{int}$ compounds (In Vivo CL$_{int,obs}$< 10 mL/min/kg)								
Warfarin	A	CYP2C9	0.55[e]	0.01	0.94	0.98	1.00	0.97
Theophylline	N	CYP1A2	0.83[b]	0.21	0.96	0.99	1.00	0.98
Tolbutamide	A	CYP2C9, CYP2C19	0.75[b]	0.02	0.83	0.95	1.00	0.91
Lorazepam	N	UGT	1.1[a]	0.08	0.85	0.96	1.00	0.92
Glipizide	A	CYP2C9	0.55[e]	0.02	0.96	0.99	1.00	0.98
Etodolac	A	UGT, CYP2C9	0.60[c]	0.01	- [¥]	0.97	1.00	0.95
Ketoprofen	A	UGT	0.55[e]	0.02	0.96	0.99	1.00	0.98
Ondansetron	B	CYP3A4	0.83[c]	0.50	0.88	0.96	1.00	0.94
intermediate to high CL$_{int,obs}$ compounds								
Chlorpromazine	B	CYP2D6	0.78[c]	0.01	0.07	0.21	0.83	0.13
Propranolol	B	CYP2D6, CYP1A2	0.83[b]	0.21	0.63	0.86	0.99	0.77
Nifedipine	N	CYP3A4	0.59[b]	0.03	0.79	0.93	1.00	0.88
Verapamil	B	CYP2C8, CYP3A4	0.84[d]	0.12	0.52	0.80	0.99	0.68
Metoprolol	B	CYP2D6	1.13[b]	0.88	0.90	0.97	1.00	0.95
Naloxone	B	UGT	1.22[b]	0.25	0.93	0.98	1.00	0.96

A acid, *B* base, *N* neutral
[¥] fraction unbound in the incubation calculated according to (28) for etodolac
*Measured fraction unbound in the incubation derived from (25) and corrected for cell concentration according to Eq. 3
[a] R_b values obtained from (34)
[b] R_b values obtained from (35)
[c] R_b values obtained from (36)
[d] R_b values obtained from (37)
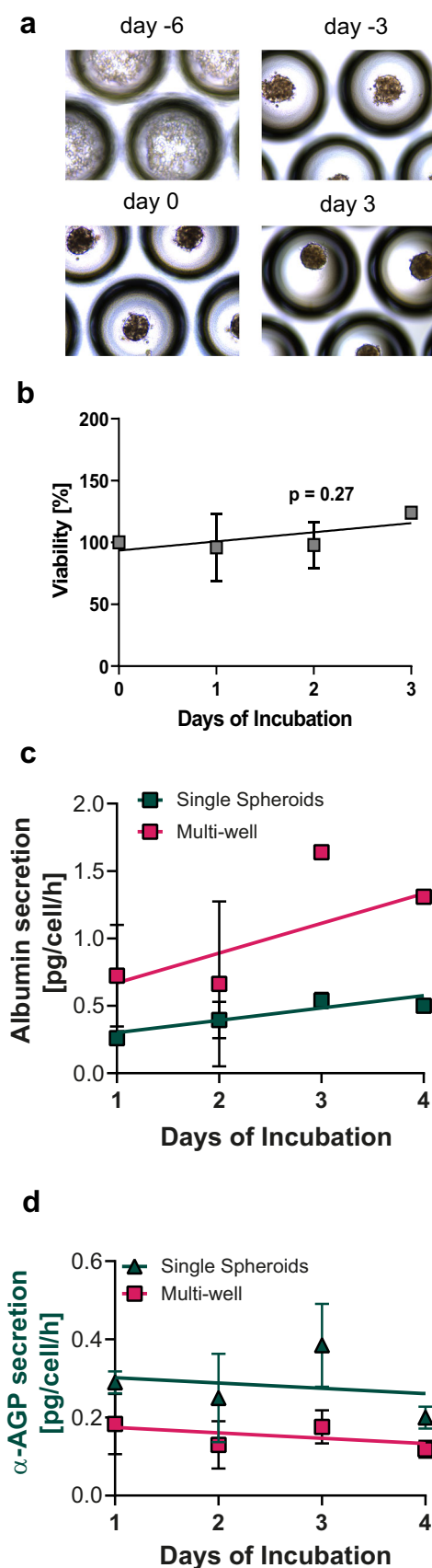[e] R_b values obtained from (38)

Fig. 1. Multi-well spheroids remain viable and functional during the drug incubation time. **a** Bright-field images of spheroid formation in multi-well plates. **b** Cellular ATP levels of multi-well spheroids over the drug incubation time. Data points represent the mean of quadruplicates ± standard deviation. **c** Albumin concentrations in the medium secreted by multi-well and single spheroids during the incubation time. Data points represent the mean of triplicates ± standard deviation. **d** α-AGP concentrations in the medium secreted by multi-well and single spheroids during the incubation time. Data points represent the mean of triplicates ± standard deviation. Deviations from linearity were calculated using F test (GraphPad Prism version 8.2.0, GraphPad Software, San Diego, USA)

equilibration at 37 °C, the compound concentration was measured using LC-MS/MS. The fu_p was determined by dividing the drug concentration in the dialysate by the concentration in the plasma. To determine the fraction unbound in blood (fu_b), the obtained fu_p was divided by the blood-to-plasma ratio (R_b) which was obtained from literature (Table II).

Data Analysis

An overview of all steps of the *in vitro in vivo* extrapolation is shown in Supplemental Fig. 1.

In vitro CL_{int} values were calculated from parent compound loss using Eq. 1:

$$Invitro\ CL_{int} = -k_e * \frac{\text{incubation volume}}{\text{seeded hepatocytes}}\ \mu L\text{*}min^{-1} * 10^6 cells^{-1}\quad (1)$$

where k_e is the elimination rate constant representing the slope of the linear regression of the natural logarithm of the percentage remaining parent compound *versus* incubation time. Deviation of the slope from 0 was tested using a F test followed by a Bonferroni-Dunn correction. In cases, where the slope was not significantly different from zero, an estimated CL_{int} was determined, using the slope calculated. From the *In vitro* CL_{int} the scaled *In vivo* CL_{int} was calculated by taking physiological scaling factors (25.7 g liver/kg body weight, 120×10^6 cells/g liver), fraction unbound in the incubation (fu_{inc}), and fu_b into account (Table II, Eq. 2).

$$\underset{\text{Invivo CL}_{int}}{\text{Scaled}} = \text{Invitro CL}_{int} * \frac{\text{liver weight}}{\text{standard body weight}} * \frac{\text{hepatocytes}}{\text{gram of liver}} * \frac{fu_b}{fu_{inc}}\quad (2)$$

The fu_{inc} was calculated from measured binding in human hepatocytes in suspension and corrected for cell density according to Eq. 3 (19).

$$fu_2 = \frac{1}{\frac{c_1}{c_2} * \left(\frac{1 - fu_1}{fu_1}\right) + 1}\quad (3)$$

For *in vivo* CL_{int} predictions (*In vivo* $CL_{int,pred}$), a regression line correction was used as described previously (20), using all values obtained, including estimated CL_{int} values for the suspension and single spheroid cultures.
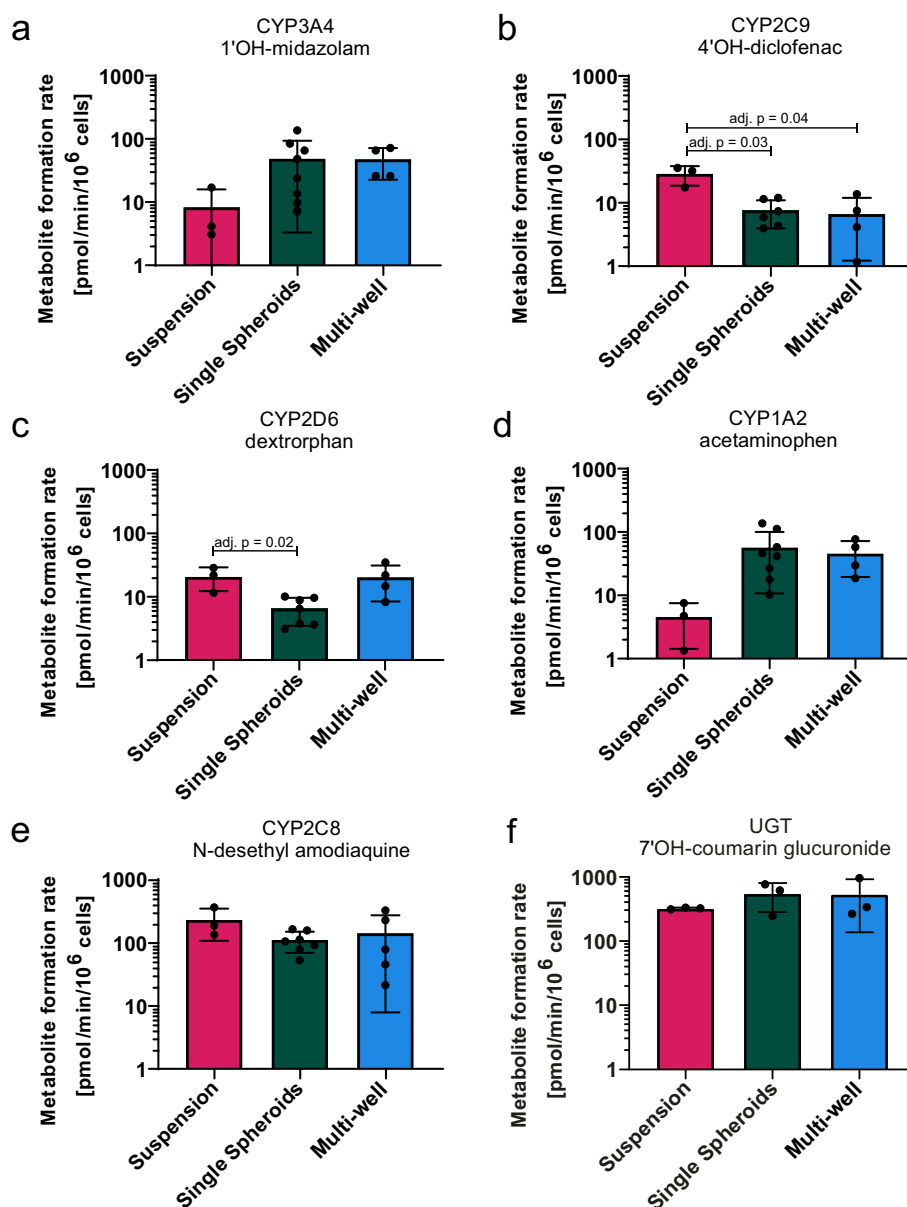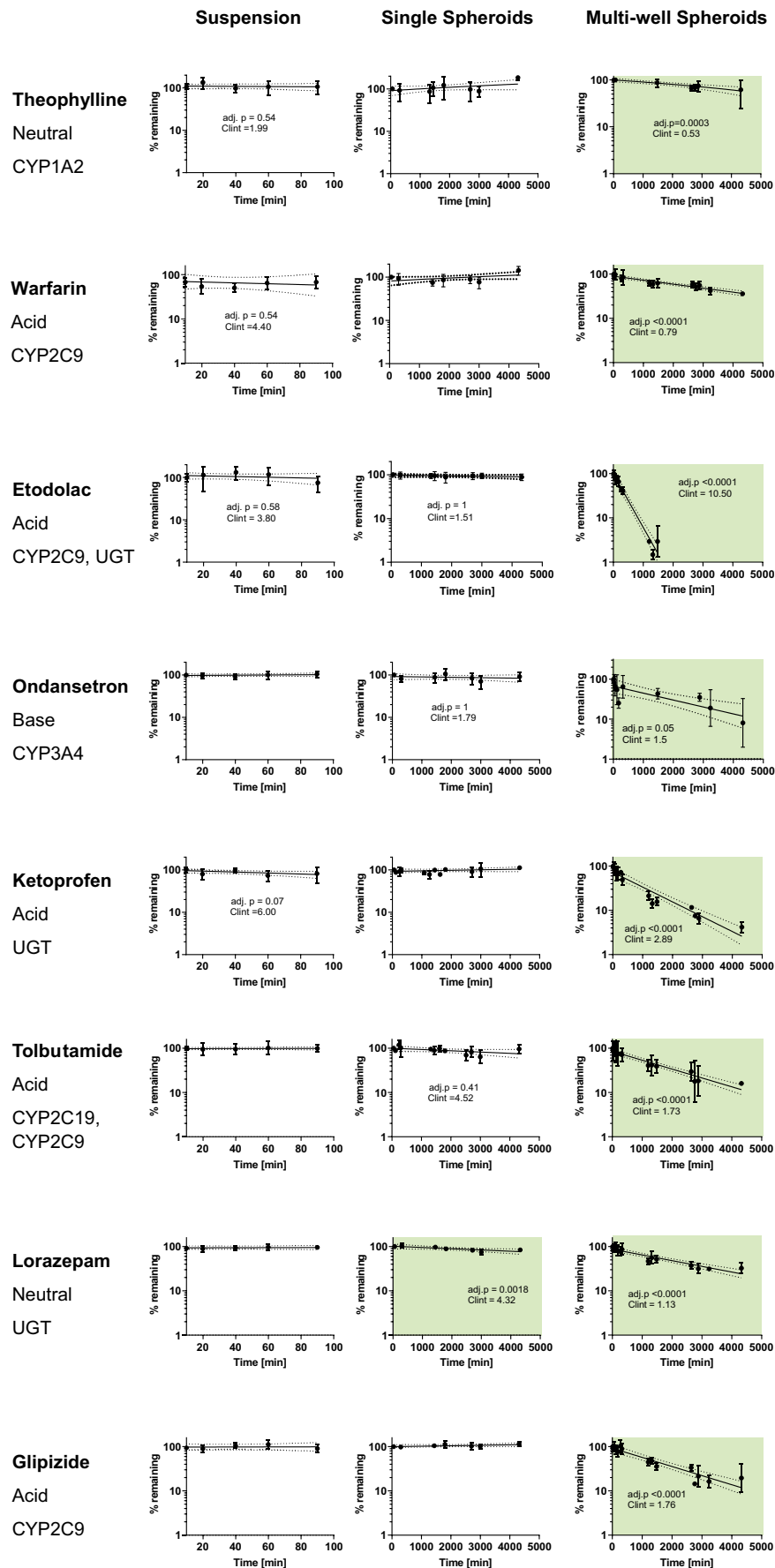
Fig. 2. Comparison of metabolic activities of suspension, single, and multi-well spheroid cultures. **a** CYP3A4 activity shown as formation of 1'OH-midazolam after midazolam treatment. **b** CYP2C9 activity shown as formation of 4'OH-diclofenac after diclofenac treatment. **c** CYP2D6 activity shown as formation of dextrorphan after dextromethorphan treatment. **d** CYP1A2 activity shown as formation of acetaminophen after phenacetin treatment. **e** CYP2C8 activity shown as formation of N-desethyl amodiaquine after amodiaquine treatment. **f** UGT activity shown as formation of 7'OH-coumarin glucuronide after 7'OH-coumarin treatment. Each datapoint represents an independent experiment with $n = 2$ incubations. The bars represent the mean of all datapoints ± standard deviation. A one-way ANOVA followed by a Tukey-Kramer test was performed (GraphPad Prism version 8.2.0, GraphPad Software, San Diego, USA). Significant (< 0.05) adj. p values are reported

In order to compare the prediction accuracy of CL_{int} for intermediate to high clearance compounds, a leave one out cross-validation (LOOCV) was performed for each system. Here, all compounds but one were used as a training set, resulting in a specific regression correction factor. With this factor, the CL_{int} value of the left-out compound was corrected. This procedure was repeated for each compound and the resulting absolute fold error was calculated.

Using the well-stirred model (WSM) and the *In vivo* $CL_{int,pred}$, the predicted *In vivo* clearance ($CL_{b, pred}$) was determined (Eq.4) with Q_h being the liver blood flow (20 mL/min/kg).

$$\textit{Invivo } CL_{b,pred} = \frac{\textit{Invivo } CL_{int,pred} * Q_h}{Q_h + \textit{Invivo } CL_{int,pred}} \tag{4}$$

	Suspension	Single Spheroids	Multi-well Spheroids

Theophylline
Neutral
CYP1A2

Suspension: adj. p = 0.54, Clint =1.99
Single Spheroids:
Multi-well Spheroids: adj.p=0.0003, Clint = 0.53

Warfarin
Acid
CYP2C9

Suspension: adj. p = 0.54, Clint =4.40
Multi-well Spheroids: adj.p <0.0001, Clint = 0.79

Etodolac
Acid
CYP2C9, UGT

Suspension: adj. p = 0.58, Clint = 3.80
Single Spheroids: adj. p = 1, Clint =1.51
Multi-well Spheroids: adj.p <0.0001, Clint = 10.50

Ondansetron
Base
CYP3A4

Single Spheroids: adj.p = 1, Clint =1.79
Multi-well Spheroids: adj.p = 0.05, Clint = 1.5

Ketoprofen
Acid
UGT

Suspension: adj. p = 0.07, Clint =6.00
Multi-well Spheroids: adj.p <0.0001, Clint = 2.89

Tolbutamide
Acid
CYP2C19,
CYP2C9

Single Spheroids: adj.p = 0.41, Clint =4.52
Multi-well Spheroids: adj.p <0.0001, Clint = 1.73

Lorazepam
Neutral
UGT

Single Spheroids: adj.p = 0.0018, Clint = 4.32
Multi-well Spheroids: adj.p <0.0001, Clint = 1.13

Glipizide
Acid
CYP2C9

Multi-well Spheroids: adj.p <0.0001, Clint = 1.76

The observed *In vivo* clearance (*In vivo* $CL_{b,\,obs}$) was obtained from the *In vivo* plasma clearance (*In vivo* $CL_{pl,\,obs}$) as described in Eq. 5.

$$In vivo\ CL_{b,obs} = \frac{In vivo\ CL_{pl,obs}}{R_b} \tag{5}$$

The observed *In vivo* CL_{int} (*In vivo* $CL_{int,\,obs}$) was derived from the *In vivo* $CL_{b,\,obs}$ using the WSM (Eq. 6).

$$In vivo\ CL_{int,obs} = \frac{In vivo\ CL_{b,obs} * Q_h}{Q_h - In vivo\ CL_{b,obs}} \tag{6}$$

The prediction accuracy for *In vivo* CL_b was calculated using the absolute average fold error (AAFE) according to Eq. 7, where N represents the number of compounds.

$$AAFE = 10^{\frac{\Sigma \left| \log \frac{CL_{b,pred}}{CL_{b,obs}} \right|}{N}} \tag{7}$$

The incubation factor of different *in vitro* models was calculated as shown in Eq. 8.

$$Incubation\ factor = incubation\ time * cell\ concentration\ \frac{min * 10^6 cells}{mL} \tag{8}$$

RESULTS

Spheroids formed in micro-well arrays resulted in approximately 80 spatially separated spheroids of homogeneous size (500 PHH per spheroid) per macrowell. The kinetics of spheroids formation were similar to those in conventional single spheroid culture, taking around 6 days for the aggregation of the seeded cell suspension into spheroids with well-defined perimeters and stable morphology (Fig. 1a). Notably, viability and hepatocyte functionality as indicated by ATP measurements and albumin and α-AGP secretion, remained stable over the experimental time (Fig. 1b–d). Albumin and α-AGP secretion per cell and hour were comparable between multi-well spheroids and single spheroids (Fig. 1c, d). Furthermore, suspension, single spheroid, and multi-well spheroid cultures showed similar metabolic activity. CYP3A4 and CYP1A2 trended (not statistically significant) toward higher activities in both spheroid systems compared to isogenic suspension cultures. Tendencies were inverted for CYP2C9 with significant differences between suspension and single spheroid or multi-well cultures (adj. *p* =

◄ **Fig. 3** Substrate depletion plots of eight low clearance compounds from suspension, single and multi-well spheroid cultures. Data points represent mean of triplicates (suspension, single spheroids) or quadruplicates (multi-well spheroids) ± standard deviation. CL_{int} values are given as µL/min/10^6 cells. Dotted lines represent the 95% confidence interval. Deviations from linearity were calculated using F test (GraphPad Prism version 8.2.0, GraphPad Software, San Diego, USA) with a post-hoc Bonferroni-Dunn test. Graphs are highlighted in green when slope was significantly different from zero

0.03 and 0.04, respectively; Fig. 2). CYP2D6 activity was slightly reduced in single spheroids but not in multi-well spheroids compared to suspension cultures (adj. *p* = 0.02). For uridine 5′-diphospho-glucuronosyltransferases (UGT) the activity was similar between the different systems (Fig. 2).

To compare the utility of the different systems for low CL_{int} measurements, we next measured the clearance of eight slowly metabolized compounds (Fig. 3). For suspension cultures, significant turnover could not be measured for any of these compounds. However, four out of eight compounds showed a negative slope, which allowed estimation of CL_{int}. In single spheroids, significant turnover was observed for lorazepam only (CL_{int} = 4.3 µL/min/10^6 cells; adj. *p* = 0.0018) but the resulting *in vivo* $CL_{int,pred}$ exceeded the human *in vivo* $CL_{int,obs}$ by 9-fold (Table III) and $CL_{b,\,obs}$ by 7-fold (Table IV). Three additional compounds (etodolac, ondansetron, and tolbutamide) allowed CL_{int} estimation, while the remaining four compounds were not cleared. In stark contrast, spheroids in multi-well arrays resulted in significant (adj. *p* < 0.05) turnover of all eight tested low clearance compounds with the lowest measured CL_{int} being 0.53 µL/min/10^6cells for theophylline (Fig. 3). A comparison of the incubation factor of the three tested systems revealed a more than ten times higher incubation factor for the multi-well system compared to the single spheroid or suspension cultures. The single spheroid cultures had an approximately two times higher incubation factor compared to suspension cultures (Table V).

Next, the accuracy of all systems for predicting intrinsic clearance was assessed. Direct scaling resulted in underprediction of most of the high clearance compounds in all systems. This systematic underprediction was corrected using a linear regression based on all available CL_{int} values for each system including those CL_{int} values that could only be estimated. The accuracy of CL_{int} prediction for the high CL_{int} compounds, defined as *in vivo* $CL_{int,obs}$ higher than 10mL/min/kg, was similar for all tested culture systems, whereas for low CL_{int} compounds, the multi-well spheroids performed the best (Table III). Since for most of the low clearance compounds, only an estimated CL_{int} value or no value could be determined in suspension and single spheroids, a set of six intermediate to high clearance compounds and a LOOCV was used to further compare the prediction accuracy of the different cultures. The resulting absolute fold errors for these compounds were similar between all culture systems (Fig. 4).

Further, the predictions of CL_b using the different systems where compared (Table IV). The CL_b prediction of rapidly metabolized compounds was similar for all systems. Using the suspension culture and single spheroids, only the clearance of nifedipine was underpredicted by more than 3-fold. Additionally, the clearance of metoprolol could not be determined using single spheroids. The CL_b of all high CL_{int} compounds were predicted within 3-fold when using the multi-well system.

For the low CL_{int} compounds, the $CL_{b,obs}$ was overpredicted for two out of four compounds when suspension or single spheroids were used. Overall, CL_b predictions using the multi-well system were within 2-fold and 3-fold for 86% (12/14) and 93% (13/14) of all tested compounds, respectively. Two compounds were predicted outside 2-fold: the neutral compound theophylline was overpredicted by 3.7-fold and the basic compound chlorpromazine was underpredicted by 2.04-fold. This resulted in an AAFE of

1.24 (Fig. 5, Table IV). Hence, the multi-well system allowed quantitatively accurate predictions of human *in vivo* CL_b over two orders of magnitude.

DISCUSSION

Clinical drug candidates with a low metabolic turnover have become increasingly common in drug discovery. Low clearance is a desired property as it extends half-life and overall free exposure, allowing for prolonged target engagement and ultimately lower human doses. However, the *in vitro* quantification of slow metabolic hepatic drug turnover is challenging. The current gold standard method, hepatocyte suspension culture, shows a rapid loss of CYP activity, which limits the incubation time to a few hours (2). More phenotypically stable culture methods, such as spheroids and MPCCs, allow for extended incubation times but have, in comparison to suspension cultures, relatively low cell-to-medium volume ratios which curtails their performance (Table V). Pooling of spheroids has been suggested to increase the cell-to-media ratio (17). However, Riede *et al.* reported rapid fusing upon pooling, which was paralleled by a loss of phenotype (16).Thus, in accordance with this study, while conventional PHH spheroids remain metabolically active for several days, the cell-to-media ratio is insufficient

for CL_int determination of low clearance compounds. Similar limitations apply to MPCCs. Longer incubations may partially compensate for the low hepatocyte concentration. Incubation times exceeding 1 week are however likely to be associated with practical challenges such as evaporation, nutrient depletion, and chemical instability of the compounds. Clearance quantifications of MPCC have not been directly compared to multi-well spheroids in side-by-side experiments. However, given their ~ 5-fold lower incubation factor, it can be expected that MPCC will show a higher fraction of low clearance compounds with non-significant turnover. A similar incubation factor as in multi-well cultures can be achieved by using conventional 2D co-cultures but especially the activity of CYP enzymes has been reported to be lower compared to suspension cultures (5). However, Hultman *et al.* reported similar CL_int values for seven intermediate to high clearance compounds for suspension and co-cultures (11). Hence, a comparison of the activity of drug metabolizing enzymes using donor matched cultures appears to be required to draw further conclusions.

As hepatocyte cultures from different donors differ metabolic activity, all three systems were tested using cells from the same donor to allow direct comparison. However, in order to reflect inter-donor variability in metabolic activity or to assess population averages, measurements with several

Table III. Scaled Intrinsic Clearance and Predicted *In Vivo* Intrinsic Clearance (*In Vivo* CL_int,pred) Derived from Suspension, Single Spheroid, and Multi-Well Cultures and Observed *In Vivo* Intrinsic Clearance (*In Vivo* CL_int,obs) of All Compounds. *In Vivo* CL_int,obs was calculated from plasma Clearance (CL_pl) values from literature according to Eq. 5 and Eq. 6. Blue and red marked values represent 3-fold under- and overprediction, respectively

Compound	*In Vivo* CL_int, obs [mL/min/kg]	Scaled CL_int [mL/min/kg]			*In Vivo* CL_int,pred [mL/min/kg]		
		Suspension	Single spheroid	Multi-well spheroid	Suspension[e]	Single Spheroid[f]	Multi-well Spheroids[g]
low CL_int							
Warfarin	0.30[a]	0.34[#]	N/A	0.06	3.56[#]	N/A	0.32
Theophylline	0.65[b]	1.54[#]	N/A	0.41	9.51[#]	N/A	2.63
Tolbutamide	0.46[c]	N/A	0.39[#]	0.16	N/A	4.81[#]	0.92
Lorazepam	0.95[d]	N/A	0.97	0.27	N/A	9.28	1.63
Glipizide	1.07[d]	N/A	N/A	0.15	N/A	N/A	0.87
Etodolac	1.28[a]	0.06[#]	0.02[#]	0.17	1.17[#]	0.62[#]	0.97
Ketoprofen	3.40[d]	0.54[#]	N/A	0.26	4.85[#]	N/A	1.59
Ondansetron	10.7[d]	N/A	3.33[#]	2.98	N/A	22.6[#]	22.7
high CL_int							
Chlorpromazine	24.6[a]	3.80	1.29	1.05	17.1	11.4	7.41
Propranolol	52.2[d]	11.8	5.27	3.97	35.7	31.5	32.3
Nifedipine	32.6[d]	0.11	0.41	2.46	1.76	4.96	19.0
Verapamil	76.0[c]	7.26[#]	3.04	2.22	26.0[#]	21.2	17.0
Metoprolol	28.6[c]	15.3	N/A	11.2	42.1	N/A	101
Naloxone	79.6[a]	6.17	14.3	10.2	23.4	64.7	90.9

N/A not applicable as no turnover (positive slope) was measured, marked in grey

[a] Plasma clearance values obtained from (32)

[b] Plasma clearance values obtained from (20)

[c] Plasma clearance values obtained from (39)

[d] Plasma clearance values obtained from (40)

[e] Regression correction using $\log(CL_{int}) = 0.6x + 0.86$

[f] Regression correction using $\log(CL_{int}) = 0.7x + 0.98$

[g] Regression correction using $\log(CL_{int}) = 1.1x + 0.85$

[#] Regression slope not significantly different from zero but negative

Table IV. Observed and Predicted *In Vivo* Clearance (CL$_b$) for All Three Systems After Linear Regression Correction. red marked values represent 3-fold under- and overprediction, respectively

Compound	CL$_{b, obs}$ [mL/min/kg]	CL$_{b, pred}$ [mL/min/kg]		
		Suspension	Single spheroid	Multi-well spheroids
low CL$_{int}$				
Warfarin	0.28[a]	3.02[#]	N/A	0.31
Theophylline	0.63[b]	6.45[#]	N/A	2.32
Tolbutamide	0.45[c]	N/A	3.87[#]	0.88
Lorazepam	0.91[d]	N/A	6.34	1.51
Glipizide	1.02[d]	N/A	N/A	0.83
Etodolac	1.20[a]	1.11[#]	0.61[#]	0.92
Ketoprofen	2.71[d]	3.90[#]	N/A	1.48
Ondansetron	6.99[d]	N/A	10.6[#]	10.6
high CL$_{int}$				
Chlorpromazine	11.0[a]	9.21	7.26	5.41
Propranolol	14.5[d]	12.8	12.2	12.4
Nifedipine	12.4[d]	1.62	3.98	9.75
Verapamil	15.8[c]	11.3[#]	10.3	9.18
Metoprolol	11.8[c]	13.6	N/A	16.7
Naloxone	15.9[a]	10.8	15.3	16.4

N/A not applicable as no turnover was measured (positive slope), marked in grey
[a] Plasma clearance values obtained from (32)
[b] Plasma clearance values obtained from (20)
[c] Plasma clearance values obtained from (39)
[d] Plasma clearance values obtained from (40)
[#] Regression slope not significantly different from zero but negative

donors are needed. This can be accomplished by using individual donor replicates or by using pooled donor lots for spheroids formation; however, the latter requires suitable lots for spheroid formation and monitoring of hepatocyte integration from all donors. Besides this shortcoming, multi-well spheroids address several limitations of the other systems discussed above. Firstly, spheroids remained spatially separated, avoiding fusion and dedifferentiation. Spheroids in the multi-well system consist of approximately 500 cells, whereas 1500 cells were used for single spheroid cultures. Previous work by us and others indicated that cell number had, if at all, only marginal impacts on cellular function and metabolic activity (12, 21). Furthermore, it was shown that per-cell uptake and metabolism even of polar molecules, such as glucose does not differ between spheroid sizes of 500 to 1500 cells (22). However, as uptake mechanisms differ between compounds, effects of spheroid size on drug disposition and metabolism remain to be determined. Secondly, albumin and α-AGP secretion remained constant and were similar to single spheroids. Importantly, the secretion of multi-well spheroids was comparable to *in vivo* rates, demonstrating their phenotypic stability (23, 24). Further, the cell-to-media ratio was higher than in other systems with unambiguous stable phenotypic expression of drug metabolizing enzymes.

Importantly, spheroids in multi-well arrays enabled accurate quantification of turnover of all tested compounds, including those with low, intermediate, and high clearance. In line with previous reports, all systems underpredicted the *in vivo* CL$_{int}$ when scaled without correction (20, 25, 26). The underlying root cause of this underestimation, which appears to be present regardless of the *in vitro* system used, is currently a subject to debate (10, 27). Several methods have

Table V. Incubation Time, Cell Concentration and Incubation Factor of Suspension, Single Spheroid, and Multi-Well Spheroid Cultures, as well as MPCC and 2D Co-Cultures with Information From Literature

Cell system	Incubation Time [min]	Hepatocyte Concentration [10^6 cells/mL]	Incubation Factor [min*10^6 cells/mL]
Suspension	90	0.5	45
Single spheroids	4320	0.021	91
Multi-well spheroids	4320	0.27	1166
MPCC*	4740	0.05	237
2D Co-culture#	4320	0.31	1339

[*] Using culture information from (41)
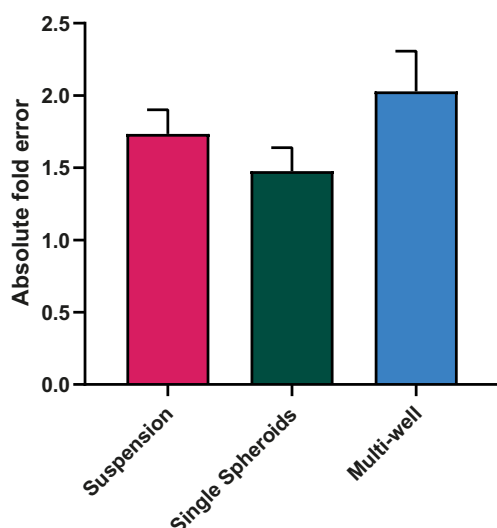[#] Using culture information from (6)

Fig. 4. Absolute fold errors for high clearance compounds after a leave one out cross validation. Values are represented as mean ± SD

been suggested to address the systematic underestimation ([28–30]). In the current study, we used the purely empirical regression offset approach similar to other reports focused on low clearance compounds ([6, 17]). This resulted in a prediction within 3-fold for 60%, 56%, and 71% of the measurable compounds for suspension, single spheroid, and multi-well cultures, respectively. A prediction within 2-fold was obtained for 50%, 22%, and 43% of the compounds for suspension, single spheroid, and multi-well cultures, respectively. Using the relay method and direct scaling, intrinsic clearance could be predicted within 2-fold for 64% and within 3-fold for 82% of the in total eleven tested compounds ([4, 31]). In 2D co-cultures, intrinsic clearance was predicted within 3-fold or 2-fold for 70% and 45% of 20 tested compounds, respectively ([11]). Hence, the prediction accuracy of CL_{int} using multi-well

cultures was similar compared to other culture systems previously used for low clearance compounds.

The extrapolated CL_b was predicted within 2-fold and 3-fold for 86% and 93% of the tested compounds, respectively when using multi-well cultures. The AAFE was 1.24. Similar accuracies have been reported using suspension hepatocytes using a regression correction ([20, 26, 32]). Also with MPCCs, CL_b was predicted within 2-fold for 70% and within 3-fold for 100% of the 10 tested low clearance drugs ([33]), while single spheroids achieved CL_b predictions within 3-fold for 86% of seven tested compounds with an AAFE of 1.74 ([16]).

Hence, multi-well spheroids present a novel *in vitro* tool for measurements and CL_b prediction and present an alternative method for clearance predictions with particular utility for slowly metabolized compounds.

CONCLUSION

Multi-well spheroids showed a similar metabolic activity as single spheroids and suspension cultures. This system was successfully used for long-term intrinsic clearance studies of slowly metabolized compounds. The high cell concentration combined with the stable metabolic activity over a long incubation time resulted in superior detection of CL_{int} compared to suspension and single spheroid cultures. Prediction of *in vivo* CL_b resulted in overall good accuracy. Thus, multi-well spheroids present a novel and valuable addition to the ADME *in vitro* tool kit.

SUPPLEMENTARY INFORMATION

AUTHORS CONTRIBUTION

Participated in research design: Georgi, Lauschke, Petersson and Preiss. Conducted experiments: Preiss.
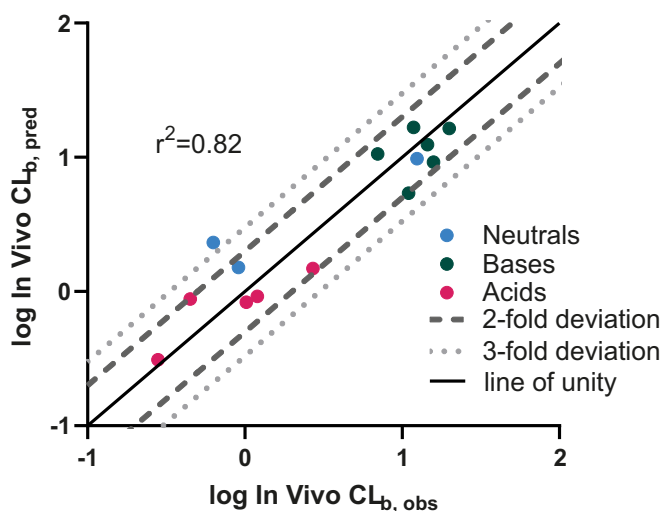

Fig. 5. Correlation of predicted and observed CL_b data using the multi-well system. Data points represent the CL_b values obtained from multi-well cultures. Blue represents neutrals, green bases, and pink acids. The dotted and dashed lines represent the 3-fold and 2-fold deviation, respectively. The black solid line represents the line of unity

Performed data analysis: Preiss. Interpretation of data: Lauschke, Petersson, and Preiss. Wrote or contributed to the writing of the manuscript: Georgi, Lauschke, Petersson, and Preiss.

DECLARATIONS

Conflict of Interest Katrin Georgi, Lena C. Preiss, and Carl Petersson were employed by the healthcare business of Merck KGaA (Darmstadt, Germany) when this study was conducted. Volker M. Lauschke is co-founder, CEO, and shareholder of HepaPredict AB, and co-founder and shareholder PersoMedix AB. In addition, Volker M. Lauschke discloses consultancy work for EnginZyme AB. The authors have no relevant additional financial interests.

REFERENCES

1. Di L, Obach RS. Addressing the Challenges of Low Clearance in Drug Research. AAPS J. 2015;17:352–7.
2. Smith CM, Nolan CK, Edwards MA, Hatfield JB, Stewart TW, Ferguson SS, Lecluyse EL, Sahi J. A comprehensive evaluation of metabolic activity and intrinsic clearance in suspensions and monolayer cultures of cryopreserved primary human hepatocytes. J Pharm Sci. 2012;101:3989–4002.
3. Stringer R, Nicklin PL, Houston JB. Reliability of human cryopreserved hepatocytes and liver microsomes as in vitro systems to predict metabolic clearance. Xenobiotica. 2008;38:1313–29.
4. Di L, Trapa P, Obach RS, Atkinson K, Bi YA, Wolford AC, et al. A novel relay method for determining low-clearance values. Drug Metab Dispos. 2012;40:1860–5.
5. Kratochwil NA, Meille C, Fowler S, Klammers F, Ekiciler A, Molitor B, et al. Metabolic Profiling of Human Long-Term Liver Models and Hepatic Clearance Predictions from In Vitro Data Using Nonlinear Mixed-Effects Modeling. AAPS J. 2017;19:534–50.
6. Bonn B, Svanberg P, Janefeldt A, Hultman I, Grime K. Determination of Human Hepatocyte Intrinsic Clearance for Slowly Metabolized Compounds: Comparison of a Primary Hepatocyte/Stromal Cell Co-culture with Plated Primary Hepatocytes and HepaRG. Drug Metab Dispos. 2016;44:527–33.
7. Yadav J, El Hassani M, Sodhi J, Lauschke VM, Hartman JH, Russell LE. Recent developments in in vitro and in vivo models for improved translation of preclinical pharmacokinetics and pharmacodynamics data. Drug Metab Rev Taylor & Francis. 2021;53:207–33.
8. Lauschke VM, Shafagh RZ, Hendriks DFG, Ingelman-Sundberg M. 3D Primary Hepatocyte Culture Systems for Analyses of Liver Diseases, Drug Metabolism, and Toxicity: Emerging Culture Paradigms and Applications. Biotechnol J. 2019;14:1–12.
9. Lauschke VM, Hendriks DFG, Bell CC, Andersson TB, Ingelman-Sundberg M. Novel 3D Culture systems for studies of human liver function and assessments of the hepatotoxicity of drugs and drug candidates. Chem Res Toxicol. 2016;29:1936–55.
10. Sodhi JK, Benet LZ. Successful and unsuccessful prediction of human hepatic clearance for lead optimization. J Med Chem. 2021;64:3546–59.
11. Hultman I, Vedin C, Abrahamsson A, Winiwarter S, Darnell M. Use of HµREL human coculture system for prediction of intrinsic clearance and metabolite formation for slowly metabolized compounds. Mol Pharm. 2016;13:2796–807.
12. Bell CC, Hendriks DFG, Moro SML, Ellis E, Walsh J, Renblom A, et al. Characterization of primary human hepatocyte spheroids as a model system for drug-induced liver injury, liver function and disease. Sci Rep. 2016;6:1–13.
13. Vorrink SU, Ullah S, Schmidt S, Nandania J, Velagapudi V, Beck O, Ingelman-Sundberg M, Lauschke VM. Endogenous and xenobiotic metabolic stability of primary human hepatocytes in long-term 3D spheroid cultures revealed by a combination of targeted and untargeted metabolomics. FASEB J. 2017;31:2696–708.
14. Ingelman-Sundberg M, Lauschke VM. 3D human liver spheroids for translational pharmacology and toxicology. Basic Clin Pharmacol Toxicol. 2021;130:1–11.
15. Mizoi K, Arakawa H, Yano K, Koyama S, Kojima H, Ogihara T. Utility of three-dimensional cultures of primary human hepatocytes (spheroids) as pharmacokinetic models. Biomedicines. 2020;8.
16. Riede J, Wollmann BM, Molden E, Ingelman-Sundberg M. Primary human hepatocyte spheroids as an in vitro tool for investigating drug compounds with low clearance. Drug Metab Dispos. 2021;49:501–8.
17. Kanebratt KP, Janefeldt A, Vilén L, Vildhede A, Samuelsson K, Milton L, Björkbom A, Persson M, Leandersson C, Andersson TB, Hilgendorf C. Primary human hepatocyte spheroid model as a 3D in vitro platform for metabolism studies. J Pharm Sci. 2021;110:422–31.
18. Zanelli U, Michna T, Petersson C. Determination of low intrinsic clearance in vitro: the benefit of a novel internal standard in human hepatocyte incubations. Xenobiotica. 2018;0:1–7.
19. Austin RP, Barton P, Cockroft SL, Wenlock MC, Riley RJ. The influence of nonspecific microsomal binding on apparent intrinsic clearance, and its prediction from physicochemical properties. Drug Metab Dispos. 2002;30:1497–503.
20. Sohlenius-Sternbeck A-K, Jones C, Ferguson D, Middleton BJ, Projean D, Floby E, et al. Practical use of the regression offset approach for the prediction of in vivo intrinsic clearance from hepatocytes. Xenobiotica. 2012;42:841–53.
21. Handin N, Mickols E, Ölander M, Rudfeldt J, Blom K, Nyberg F, et al. Conditions for maintenance of hepatocyte differentiation and function in 3D cultures. iScience. 2021;24:103235.
22. Kemas AM, Youhanna S, Zandi Shafagh R, Lauschke VM. Insulin-dependent glucose consumption dynamics in 3D primary human liver cultures measured by a sensitive and specific glucose sensor with nanoliter input volume. FASEB J. 2021;35:1–15.
23. Török E, Lutgehetmann M, Bierwolf J, Melbeck S, Düllmann J, Nashan B, et al. Primary human hepatocytes on biodegradable poly(l-Lactic acid) matrices: a promising model for improving transplantation efficiency with tissue engineering. Liver Transplant. 2011;17:104–14.
24. Colombo S, Buclin T, Décosterd LA, Telenti A, Furrer H, Lee BL, Biollaz J, Eap CB, Swiss HIV Cohort Study. Orosomucoid (α1-acid glycoprotein) plasma concentration and genetic variants: effects on human immunodeficiency virus protease inhibitor clearance and cellular accumulation. Clin Pharmacol Ther. 2006;80:307–18.
25. Wood FL, Houston JB, Hallifax D. Clearance prediction methodology needs fundamental improvement: Trends common to rat and human hepatocytes/microsomes and implications for experimental methodology. Drug Metab Dispos. 2017;45:1178–88.
26. Yamagata T, Zanelli U, Gallemann D, Perrin D, Petersson C, Yamagata T, et al. Comparison of methods for the prediction of human clearance from hepatocyte intrinsic clearance for a set of reference compounds and an external evaluation set Comparison of methods for the prediction of human clearance from hepatocyte intrinsic clearance. Xenobiotica. 2017;8254:741–51.
27. Rowland M, Roberts MS, Pang KS. In defense of current concepts and applications of clearance in drug development and therapeutics. Drug Metab Dispos. 2021;50:187–90.
28. Kilford PJ, Gertz M, Houston JB, Galetin A. Hepatocellular binding of drugs: correction for unbound fraction in hepatocyte

incubations using microsomal binding or drug lipophilicity data. Drug Metab Dispos. 2008;36:1194–7.

29. Poulin P. Prediction of total hepatic clearance by combining metabolism , transport , and Permeability data in the in vitro – in vivo extrapolation methods : Emphasis on an Apparent Fraction. J Pharm Sci. 2013;102:2085–95.

30. Hallifax D, Houston JB. Use of segregated hepatocyte scaling factors and cross-species relationship to resolve clearance-dependency in prediction of human hepatic clearance. Drug Metab Dispos. 2019;47:320–7.

31. Di L, Feng B, Goosen TC, Lai Y, Steyn SJ, Varma M V, *et al*. A perspective on the prediction of drug pharmacokinetics and disposition in drug research and development. Drug Metab Dispos. 2013;1975–93.

32. Riley RJ, McGinnity DF, Austin RP. A unified model for predicting human hepatic, metabolic clearance from in vitro intrinsic clearance data in hepatocytes and microsomes. Drug Metab Dispos. 2005;33:1304–11.

33. Chan TS, Yu H, Moore A, Khetani SR, Tweedie D. Meeting the challenge of predicting hepatic clearance of compounds slowly metabolized by cytochrome P450 using a novel hepatocyte model. HepatoPac. Drug Metab Dispos. 2018;47:58–66.

34. Deguchi T, Watanabe N, Kurihara A, Igeta K, Ikenaga H, Fusegawa K, Suzuki N, Murata S, Hirouchi M, Furuta Y, Iwasaki M, Okazaki O, Izumi T. Human pharmacokinetic prediction of UDP-glucuronosyltransferase substrates with an animal scale-up approach. Drug Metab Dispos. 2011;39:820–9.

35. Brown HS, Griffin M, Houston JB. Evaluation of cryopreserved human hepatocytes as an alternative in vitro system to microsomes for the prediction of metabolic clearance. Drug Metab Dispos. 2007;35:293–301.

36. Paixão P, Gouveia LF, Morais JAG. Prediction of drug distribution within blood. Eur J Pharm Sci. 2009;36:544–54.

37. Rodgers T, Rowland M. Mechanistic approaches to volume of distribution predictions: Understanding the processes. Pharm Res. 2007;24:918–33.

38. Sohlenius-Sternbeck AK, Afzelius L, Prusis P, Neelissen J, Hoogstraate J, Johansson J, Floby E, Bengtsson A, Gissberg O, Sternbeck J, Petersson C. Evaluation of the human prediction of clearance from hepatocyte and microsome intrinsic clearance for 52 drug compounds. Xenobiotica. 2010;40:637–49.

39. Hallifax D, Foster JA, Houston JB. Prediction of human metabolic clearance from in vitro systems: retrospective analysis and prospective view. Pharm Res. 2010;27:2150–61.

40. Obach RS, Lombardo F, Waters NJ. Trend analysis of a database of intravenous pharmacokinetic parameters in humans for 670 drug compounds. Drug Metab Dispos. 2008;36:1385–405.

41. Da-silva F, Boulenc X, Vermet H, Compigne P, Gerbal-Chaloin S, Daujat-Chavanieu M, et al. Improving prediction of metabolic clearance using quantitative extrapolation of results obtained from human hepatic micropatterned cocultures model and by considering the impact of albumin binding. J Pharm Sci. 2018;107:1957–72.